39.3/067

Ceduna-1 Second Survey

M.Kesteven & B. Parsons

June 25, 1997

1 Summary

This second study of the Ceduna-1 antenna was designed to investigate the intrinsic surface accuracy of the panels, and to assess the deformation of the antenna as it tips from the zenith to the horizon. The results are very encouraging. The panels are within the manufacturer's original specification, with an rms below 0.4mm. The gravitational deformations are also modest; relative to a surface set at a rigging elevation of 60 degrees the surface error at the elevation extremes is $<$ 1mm (rms).

notation The results described below are referenced to a coordinate frame attached to the central hub. The "z-axis" is parallel to the reflector's optical axis; the upper tripod leg is labelled *azimuth 0*, or North; positive azimuth is clockwise when looking into the dish from the subreflector.

2 The Panel Accuracy

Our earlier survey (Kesteven & Parsons - 1996) used just two targets on every second panel in order to determine the overall reflector characteristics, working on the assumption that each target was fairly representative of the actual panel surface. The present survey was designed to test that assumption by measuring the surface accuracy of the panels.

We placed a large number of targets on four adjacent panels in the second ring of panels, between radii 3 and 6 m. The targets were arranged in 9 arcs concentric with the reflector's optical axis, 144 targets in all. The position of each target relative to the design profile was determined: the distance of each target from the theodolite was measured, along with the elevation of each target. Each target was observed twice.

Figure 1 shows the raw survey data in the form of surface height profiles. The data indicate that there is some panel-to-panel variation, but this is not very different from the point-to-point variations. We can therefore obtain an upper limit to the panel accuracy by treating the ensemble as one large panel; we could get a better estimate if we processed each panel separately, and allowed for the deformation modes of a panel, but the effort does not seem warranted since the upper limit is already quite satisfactory. Table 1 summarises the results where each ring is processed separately.

The overall panel rms is 0.38 **mm**.

This analysis looked at the azimuthal variations only, as we computed, for each target, its offset from the mean elevation of all the targets in its ring. A second test compared the mean elevation of each ring with the values expected for the designed profile. After a correction for a theodolite tilt we found an rms of 0.3mm.

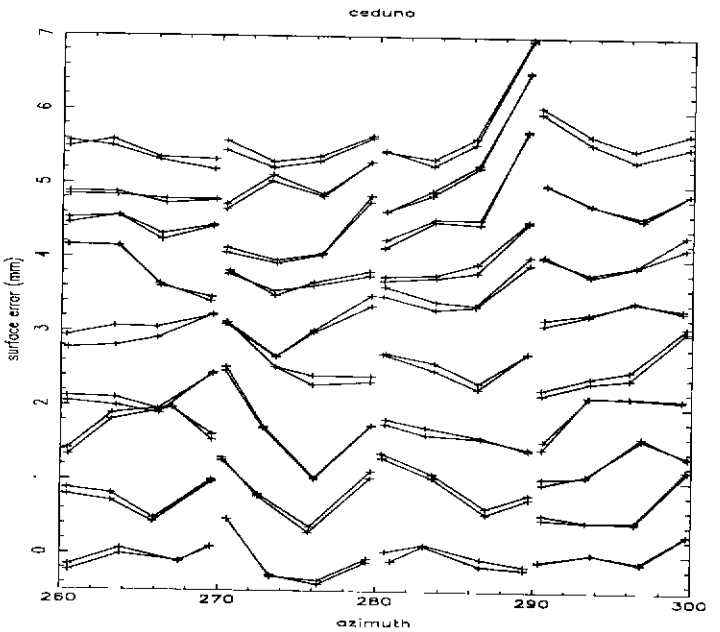

Figure 1: The raw panel data for 144 targets. The targets are arranged in 9 arcs over 4 adjacent ring 2panels. The data show each target's offset from the mean of its particular ring. Successive rings have been offset from zero for clarity

Ring #	chord length (mm)	Elevation rms (asec)	surface rms (mm)
1	3950.	11.0	0.21
2	4255.	15.3	0.31
3	4550.	17.1	0.37
4	4850.	15.9	0.37
5	5155.	18.0	0.44
6	5450.	13.1	0.34
7	5750.	16.4	0.45
8	6050.	15.6	0.45
9	6350.	13.7	0.41

Table 1: Target error sorted by target ring

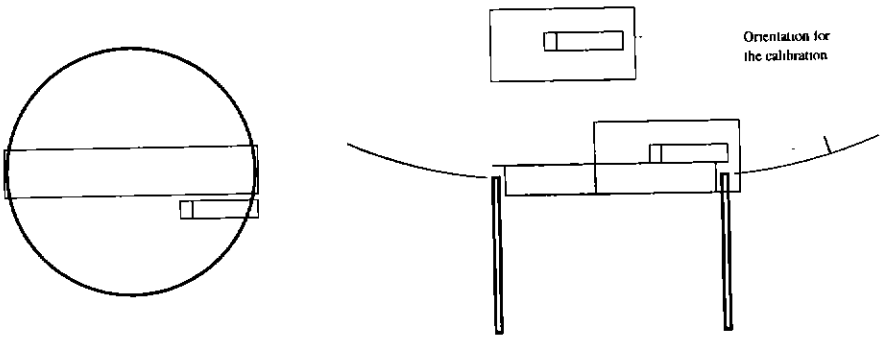

Figure 2: These views show the installation of the camera at the reflector vertex

3 The Gravitational Deformation

The experimental design was simple: a TV camera was installed near the reflector vertex, focussed on a target attached to the surface. The movement of the target in the camera's frame was observed as the antenna was driven from the zenith to the horizon. The exercise was repeated at 40 different target locations to provide a representative sampling of the reflector.

We find three effects as the antenna tips from the zenith to the horizon :

- The subreflector droops.
- The reflector surface deforms with the top edge moving upwards relative to the zenith position. The lower edge drops below the zenith position. This amounts to a rotation about the elevation axis (ie, a pointing error) and a small axial focus shift.
- There is some movement parallel to the reflector surface, most pronounced in the vicinity of the lower tripod legs. The effect has no consequences for the reflector performance.

These effects are all fairly benign when measured relative to a surface set for a rigging angle of 60 degrees.

In more detail:

3.1 The Camera and Mount

The camera was a composite assembled from a precision alignment telescope focussed onto the CCD array of a TV camera. The images were captured in a frame grabber installed in a PC.

The camera was rigidly attached to a rectangular mounting plate, which was fixed to a fabricated steel channel bolted to the central mirror support hub. (See figure 2) Calibration of this beam presented us with a number of difficulties: the beam flexed under its own weight (and so had an elevation-dependent component), and could be twisted. We placed the camera at one end of the beam near its connection to the central hub in order to minimize the warping effect; we reversed the beam and camera in order to determine the (modest) elevation component of the beam's deformation. Our conclusion, after examining the excellent repeatability of the observations and the consistency in the calibration observations, is that our results have an error of about 0.5mm.

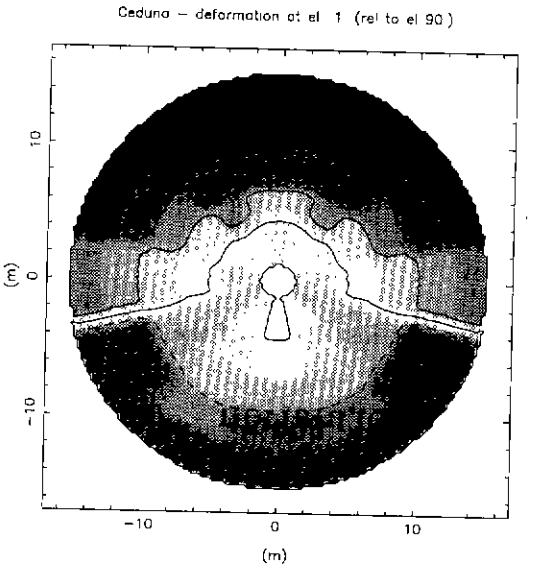

Figure 3: The target movement normal to the surface as the antenna tips from the zenith to the horizon. The gray scale shows the magnitude of shift on the scale 0 to 10mm; the contours are at 2mm spacing, and are dotted for the negative levels

3.2 The Targets

The targets were black disks placed on a reflecting background. These were fixed to a small aluminium plate which was rivetted to the panel surface The target diameter was 24mm. Our observations were made at night, with a spot-light directed at the target. The contrast between the black disk and its background was very high.

Targets were placed along eight different radial lines (at antenna azimuths 0, 30, 60, 90, 120, 150, 180 and 270 degrees) at five different radii (3, 6, 9, 12, and 15m chord lengths from the vertex). Images were captured every 15 degrees elevation starting at the zenith, both as the antenna was driving towards the horizon and on the way back.

3.3 The Processing

The processing went in three steps:

- Locate each target within its frame. Each image was clipped in order to isolate the target; a least squares search then determined the target's centre and radius. Since we know the true target diameter we can translate the target's position (in pixels) to a position in mm.

  We measured both the movement in azimuth (the x-shift) and the movement normal to the surface (the y-shift).

- The data was averaged (the "up" and the "down" observations), and sorted by elevation. We assumed symmetry about the N-S line in building the images shown below; the radial cut at 270 degrees azimuth is in agreement with the 90 degree cut, showing that the assumption is reasonable.

  Figure 3 shows the observed total y-shift between the zenith and the horizon. Figure 4 is a more realistic view, showing the effective aperture when allowance is made for for the pointing and

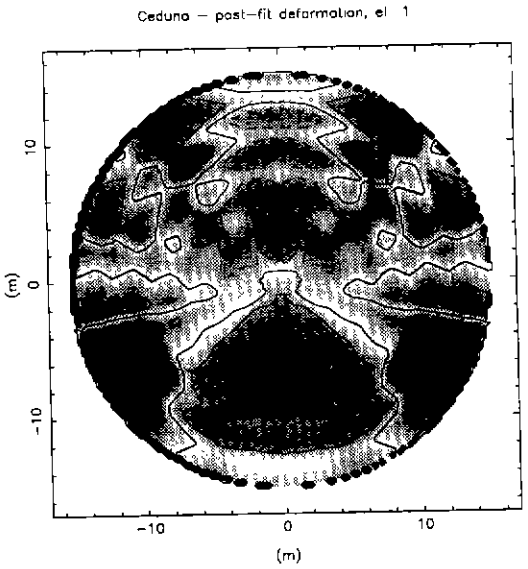

Figure 4: The target movement normal to the surface as the antenna tips from the zenith to the horizon, after correction for pointing and defocussing. The gray scale shows the magnitude of shift on the scale 0 to 5mm; the contours are at 1mm spacing, and are dotted for the negative levels

defocussing errors.

- The data was adjusted to a realistic rigging angle - 60 degrees was chosen. The y-shifts were all adjusted to be relative to the 60 degree values. An examination of the data showed a strong gradient over the aperture, probably due to a rotation of the central hub, rather than a bulk deformation of the antenna. In either case the effect is benign - at worst (bulk deformation) the antenna pointing model would require a cos(elevation) term. The deformation after correcting for the rotation contains the signature of an axial focus shift, up to 7mm at the extreme elevations. Table 2 summarises the fitting operation for each elevation.

Figure 5 shows the surface movement seen at 90 degrees (for a 60 degree rigging elevation) before allowance for the best-fit paraboloid is made. Figure 6 shows the post-fit surface.

elevation (degree)	axial focus shift (mm)	rotation (arcmin)	pre-fit rms (mm)	post-fit rms (mm)
90.	1.3	2.1	2.4	0.7
75.	0.8	1.0	1.2	0.3
60.	0.0	0.0	0.0	0.0
45.	-1.1	-0.9	1.0	0.3
30.	-3.1	-1.4	1.7	0.6
15.	-4.9	-1.8	2.2	0.8
01.	-6.9	-1.9	2.5	0.9

Table 2: Parameters of the Best Fit Paraboloid

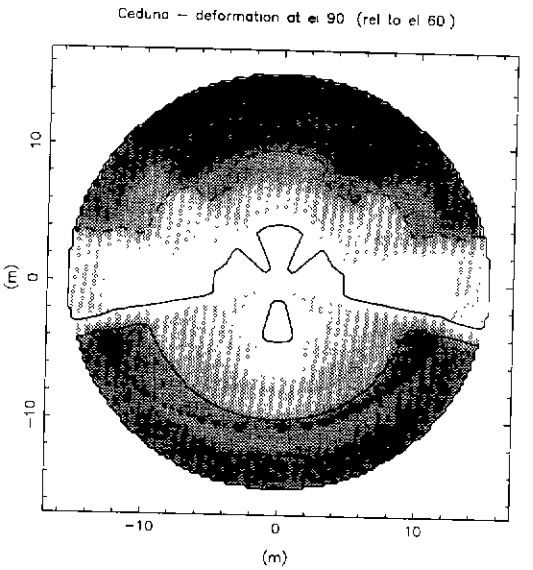

Figure 5: The 90 degree elevation surface relative to the 60 degree rigging angle surface, before the best-fit paraboloid correction. The gray scale shows the magnitude of shift on the scale 0 to 10mm; the contours are at 2mm spacing, and are dotted for the negative levels

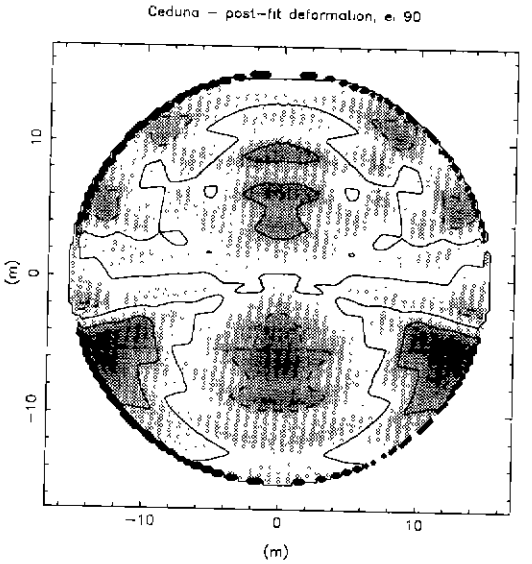

Figure 6: The 90 degree elevation surface relative to the 60 degree rigging angle surface, after the best-fit paraboloid correction. The gray scale shows the magnitude of shift on the scale 0 to 5mm; the contours are at 1mm spacing, and are dotted for the negative levels

elevation (degree)	Subreflector droop (mm)
90.	7.8
75.	3.6
60.	0.0
45.	-3.6
30.	-6.1
15.	-7.6
01.	-8.8

Table 3: The Subreflector movement as a function of elevation

elevation (degree)	offset (mm)	squint (arcmin)	total pointing error (arcmin)
90.	2.5	-0.8	1.3
75.	1.1	-0.3	0.7
60.	0.0	0.0	0.0
45.	-1.3	0.4	-0.5
30.	-2.6	1.0	-0.4
15.	-3.0	1.2	-0.6
01.	-4.0	1.3	-0.6

Table 4: The subreflector offset

3.4 Subreflector

We were able to use the same technique to measure the subreflector movement. There is a 20mm (diameter) hole in the subreflector vertex, which is a satisfactory target when viewed against the subreflector surface. The camera mount allowed us to point the camera along the reflector's optical axis. We find that the subreflector droops as the antenna tips from zenith to horizon, with a total movement of 17mm. Table 3 shows the movement referenced to the rigging angle.

Table 2 and table 3 together allow us to estimate the changing offset between subreflector and the reflector's axis. The results are given in table 4 which also includes the pointing squint implied by the offset (a beam deviation factor of 0.8 has been adopted). The "total pointing error" is the sum of the squint and the reflector rotation.

The final column in table 4 assumes that all the reflector rotation is due to a bulk deformation of the reflector; since the elevation encoder is attached to the strong central azimuthal truss, the reflector rotation would appearas a pointing error which would need to be incorporated into the control system's pointing model. On the other hand, if the observed rotation is due to the hub alone, then column 3 (the "squint") gives the pointing model, given that the hub is not a structural element rigidly connected to the encoders. Radio pointing data will clarify this problem.

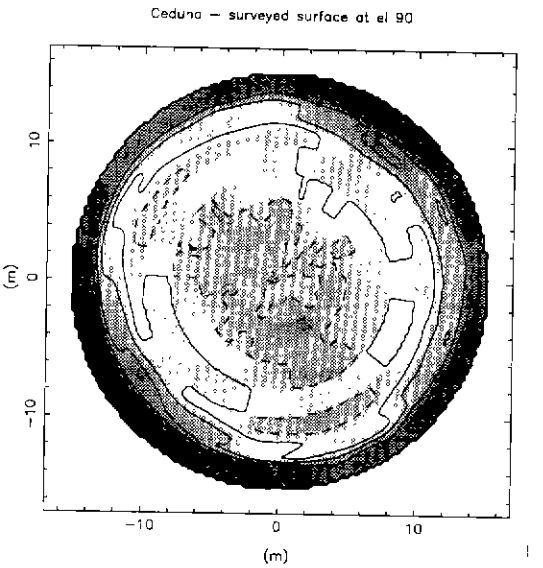

Figure 7: The surface error distribution based on the theodolite survey of October, 1997. The survey was made with the antenna at the zenith

4 The true shape of the main reflector

The antenna was surveyed in October 1996, and has been reported in AT/39.3/066 (Kesteven & Parsons). Figure 7 shows the data in a gray-scale format. There is a suggestion of astigmatism about an oblique axis; however, the main feature is the raised outer ring of panels which is 5-10mm above the profile. This would contribute to an axial defocussing effect.

This antenna was used at a very low elevation angle (for an Indian Ocean satellite), so it is perhaps surprising that we don't see the deformation signature (figure 4) in the survey data.

5 Conclusions

1. The panels have a surface accuracy of < 0.4mm (rms) which implies a 0.5 dB loss at 22GHz.
2. The gravitational deformation of the surface of ~ 0.8mm (rms) at the elevation extremes suggests a loss of up to 2 dB at 22 GHz.
3. The subreflector's axial offset could be minimised to a peak error of 4mm by optimising the focus at an elevation of about 30 degrees.
4. The subreflector's peak lateral focus offset is < 4mm. This could be reduced a bit by optimising at an elevation near 45 degrees.
5. The reflector would benefit from a panel resetting adjustment - the theodolite survey showed a surface error of 2.5mm (rms) (figure 7).

6 References

Kesteven, M.J. and Parsons, B.F. (1996) Ceduna-1 Survey, AT documemt AT/39.3/066